# All-dielectric invisibility cloaks made of $BaTiO_3$-loaded polyurethane foam



2011 New J. Phys. 13 103023

(http://iopscience.iop.org/1367-2630/13/10/103023)

New Journal of Physics
The open-access journal for physics

# All-dielectric invisibility cloaks made of $BaTiO_3$-loaded polyurethane foam

**Di Bao[1], Khalid Z Rajab[1], Yang Hao[1,3], Efthymios Kallos[1], Wenxuan Tang[1], Christos Argyropoulos[1,4], Yongzhe Piao[2] and Shoufeng Yang[2,5]**

[1] School of Electronic Engineering and Computer Science, Queen Mary University of London, London E1 4NS, UK
[2] School of Engineering and Materials Science, Queen Mary University of London, London E1 4NS, UK
E-mail: yang.hao@eecs.qmul.ac.uk

*New Journal of Physics* **13** (2011) 103023 (13pp)
Received 10 June 2011
Published 19 October 2011
Online at http://www.njp.org/
doi:10.1088/1367-2630/13/10/103023

**Abstract.** Transformation optics has led the way in the development of electromagnetic invisibility cloaks from science fiction to engineering practice. Invisibility cloaks have been demonstrated over a wide range of the electromagnetic spectrum, and with a variety of different fabrication techniques. However, all previous schemes have relied on the use of metamaterials consisting of arrays of sub-wavelength inclusions. We report on the first cloaking structure made of a high-$\kappa$ dielectric-loaded foam mixture. A polyurethane foam mixed with different ratios of barium titanate is used to produce the required range of permittivities, and the invisibility cloak is demonstrated to work for all incident angles over a wide range of microwave frequencies. This method will greatly facilitate the development and large-scale manufacture of a wide range of transformation optics-based structures.

S Online supplementary data available from stacks.iop.org/NJP/13/103023/mmedia

[3] Author to whom any correspondence should be addressed.
[4] Current address: Department of Electrical and Computer Engineering, University of Texas at Austin, Austin, TX 78712, USA.
[5] Current address: School of Engineering Science, University of Southampton, Southampton SO17 1BJ, UK.

## Contents



## 1. Introduction

Transformation optics provides the framework to manipulate electromagnetic fields, by modifying the material properties of a structure. The application of transformation optics to the burgeoning field of metamaterials has led to a number of novel applications, most notable among them being the recent pioneering work on the development of invisibility cloaks [1, 2], but also including spacetime cloaks and other time-dependent metrics [3, 4], beam manipulation [5, 6] and rotation [7], illusion optics [8, 9], superscatterers [10] and extraordinary transmission devices [11] and planar lens antennas [12–14]. An invisibility cloak is a structure that is designed to electromagnetically hide a region of space from an impinging wave within a defined part of the electromagnetic spectrum. Theoretically, coordinate transformations are applied to map the relevant region of space to a domain that would in effect appear negligible, such as a point or a line. In practice, advances in computational electromagnetics theory coupled to significant enhancements in computational processing power have enabled the numerical analysis and confirmation of the properties of these structures [15]. Recently, a number of research groups have demonstrated realizations of invisibility cloaks at microwave [16–20], terahertz [21, 22] and optical [23–26] regions of the electromagnetic spectrum. The earlier demonstrations were developed using transformation optics that led to anisotropic and spatially dispersive material properties which were composed of tensors—both electric and magnetic—with metamaterial properties that are not known to occur naturally. These metamaterials would therefore have to be created artificially using composites of substructured metallo-dielectrics that would exhibit the desired properties only at a resonant frequency. Although successful in proving the concept of the invisibility cloak, these initial realizations proved to be narrow banded and highly lossy, and certainly not ideal for any practical application. A significant breakthrough was the theoretical description of the so-called ground plane, or carpet cloak, in which the cloaked region was mapped to a line on the ground plane [27]. Perhaps most importantly, it was shown that an almost ideal version of this particular cloak can be implemented using non-magnetic, isotropic dielectrics—materials exhibiting only slight dispersion and low loss; these materials are, of course, commonly available in nature and are easily controlled and produced.

Although still spatially dispersive, the dielectric material would be discretized so that a cloaked region could be segmented into a number of blocks with a finite possibility of different permittivities. Realizations of these ground-plane cloaks were soon produced and have proven to be successful in their aim of hiding a region over a broad range of frequencies. However, these ground-plane cloaks, as with the earlier iterations of the invisibility cloak, were again formed

with sub-structured composites of metallo-dielectrics, metal–air or all-dielectrics of high-$\kappa$/low-$\kappa$ arrays. A drawback of these approaches is that, with a discretized cell that is a fraction of a wavelength in dimension, these sub-structured geometries will require micro-structuring, even at microwave frequencies where the wavelength is comparatively long. Scattering may also reduce the performance of the cloaks.

In this paper, we report on the first cloaking structure made of a high-$\kappa$ dielectric-loaded foam mixture. Polyurethane foam mixed with different ratios of barium titanate is used to produce the required range of permittivities, and the invisibility cloak is demonstrated to work for all incident angles over a wide range of microwave frequencies. The key advantages of this technique are that, due to the lack of metal or dense materials, the resulting cloaks are lightweight and low loss, and are easily fabricated. This method will greatly facilitate the development and large-scale manufacture of a wide range of transformation optics-based structures.

## 2. Cloak design

Two-dimensional (2D) ground-plane cloaks made up of spatially dispersive dielectrics have been described that effectively reduce the electromagnetic scattering signature of an object over a specific frequency band [17, 23, 24, 27]. Specifically, it was shown by Kallos *et al* [28] that the spatially dispersive dielectrics can be down-sampled to relatively few dielectric blocks, while still maintaining the overall performance characteristics of the dielectric cloak in minimizing the scattering signature of the object.

The cloak presented in this paper consists of a down-sampled selection of six dielectric blocks, with refractive indexes of 1.08, 1.14 and 1.21, corresponding to relative permittivities of 1.17, 1.30 and 1.46. In figure 1(a), the permittivity map of the dielectrics is shown, which forms a cloak that surrounds a metallic perturbation that is to be 'hidden' from the incident electromagnetic waves. The dielectric blocks are each of dimension $34.25 \times 30\,\mathrm{mm}^2$ ($1.14\lambda \times \lambda$ at 10 GHz), with the dielectric blocks in contact with the perturbation cut appropriately, as in the figure. The perturbation is an electrically large aluminium triangle with a base of 144 mm and a height of 16 mm ($b = 4.8\lambda$ and $h = 0.53\lambda$ at 10 GHz). At the base of the triangle is a metallic ground plane, and metal plates enclose the structures along the $z$-axis, in order to preserve the two-dimensionality of the system. Along the $xy$-plane the structures are surrounded by air. The fabricated cloak is shown in figure 1(b). For details of the fabrication process, see section 3.

## 3. Cloak fabrication

The first stage in the realization of the cloak is the development and full characterization of the dielectric mixtures. The requirements for the materials are that they exhibit low loss and low dispersion at microwave frequencies. Homogeneous composites of polyurethane and ceramic particles are required, with strong bonding between ceramic particles and the polymer matrix, and reasonably good mechanical properties. Additionally, composites with the requisite range of dielectric properties must be easily fabricated on demand.

A dielectric mixture of polyurethane with high-$\kappa$ barium titanate ($BaTiO_3$) was found to be suitable for this purpose. Polyurethane was used to create a low-$\kappa$ foam matrix, and $BaTiO_3$ was used to load the foam in order to increase the effective permittivity while not greatly

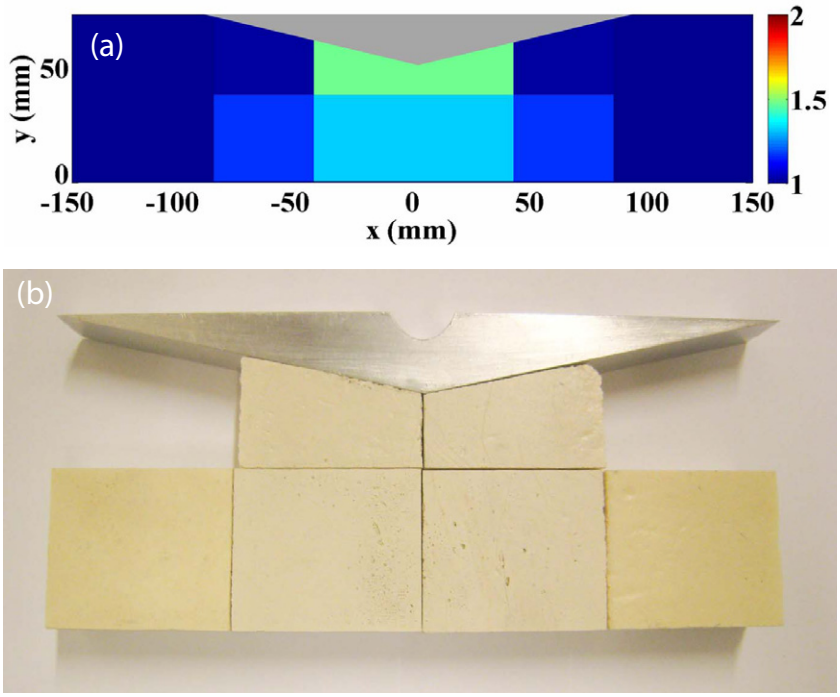


**Figure 1.** The perturbation bounded by the composite dielectrics. The perturbation is an aluminium triangle of height 16 mm and base 144 mm. At the base of the triangle is a metal boundary. In (a), the dielectric 2D map of the $4 \times 2$ blocks is shown. The dielectric blocks are rectangles of dimension $34.25 \times 30\,\text{mm}^2$. The fabricated cloak is shown in (b). In practice, a metallic ground plane is located at the base of the triangular perturbation, while the entire structure is enclosed within parallel metallic plates.

altering the mechanical properties of the structure. The density of $BaTiO_3$ powder is low, and the small particle size is advantageous when used in a dispersion system and is less likely to affect the polymer matrix structure. This results in less damage to the mechanical properties of the composite material. Both substances exhibit low loss and low dispersion at microwave frequencies, and are thus suitable for our requirements.

Samples of the composite bulk were prepared for dielectric characterization. Due to gravity, the ceramic particles tend to settle down in the composite. So the samples for analysis were cut in the middle of the composite bulk to minimize the effect of sedimentation. Knowing the weight of a sample and the weight ratio of the ceramic powder to the polyurethane used in the composite, the weight of ceramic powder in the cut sample could then be calculated. Further, if the density of the ceramic and the volume of the sample were known, the volume percentage of ceramic particles in the composite could be derived. As a result, when the permittivities of those samples were measured, the relationship between the ceramic content and the dielectric constant of the composite could be obtained. The mass quantity of $BaTiO_3$ in a sample is calculated as

$$m_{\text{BT}} = m_{\text{s}} \times \frac{m_{\text{B}}}{m_{\text{B}} + m_{\text{P}}},$$

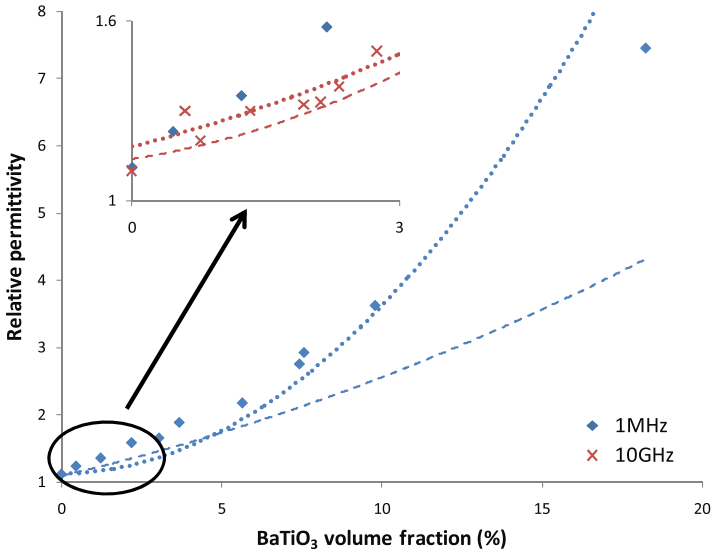


**Figure 2.** Measured relative permittivity versus $BaTiO_3$ volume fraction of the $BaTiO_3$/polyurethane composite, at 1 MHz and 10 GHz. Measured points are plotted and compared with the Maxwell–Garnett (···) and Bruggeman (- - -) effective medium relationships for three-phase mixtures.

where $m_{BT}$ is the mass of $BaTiO_3$ in the sample and $m_s$, $m_B$ and $m_P$ indicate the mass of the sample, the total input mass of $BaTiO_3$ and the input mass of polyurethane, respectively.

A range of $BaTiO_3$/polyurethane composites were fabricated in order to investigate the effects of the changing $BaTiO_3$ particle loading. In figure 2, the relative permittivity of the composite at 1 MHz and 10 GHz is plotted against the volume percentage of $BaTiO_3$. At 1 MHz, the data were obtained with an Agilent 4294 A Impedance Analyser and an Agilent 16453 parallel-plate dielectric test fixture. For characterization at 10 GHz, the samples were cut to fit an X-band waveguide. Reflection and transmission measurements were carried out with an Agilent performance network analyser, and dielectric properties were subsequently retrieved using the well-known Nicolson–Ross–Weir reflection/transmission techniques [29, 30]. It is noted that the retrieval techniques at both 1 MHz and 10 GHz are inherently broadband (from 40 Hz to 30 MHz and from 8.2 to 12.4 GHz, respectively). The measured dielectric properties were, for our purposes, dispersionless over each of these frequency ranges, and so those two frequency points were selected for representation. Furthermore, as the measured permittivities at both frequencies agree relatively well, it would imply that there is little dispersion between the bands. It is clear that a large range of permittivity values can be attained by controlling the volume percentage of $BaTiO_3$.

The requisite material samples were fabricated for the cloaking material. Recalling that the refractive indexes for the four different regions are 1.01, 1.08, 1.14 and 1.21, these correspond to relative permittivities of 1.02, 1.17, 1.30 and 1.46. The first region is represented by air, while polyurethane/$BaTiO_3$ composites were fabricated for three other higher-permittivity regions. The measured permittivities of the samples are shown in the inset to figure 2. The measured permittivities showed very good agreement with the specified values, with errors of up to about 2%.

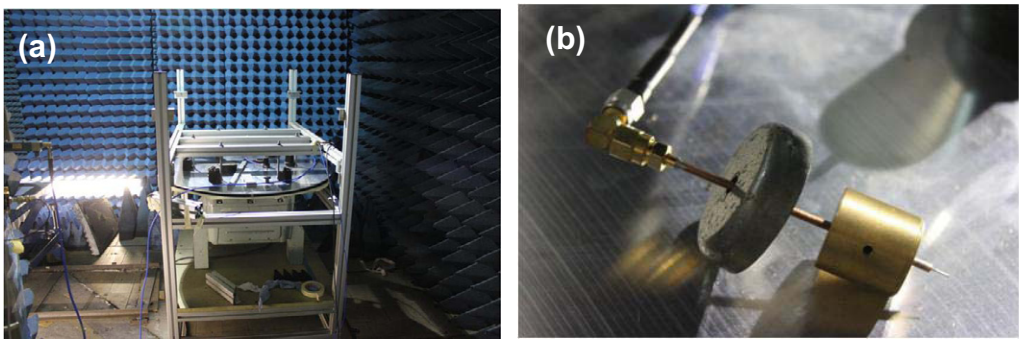


**Figure 3.** The cloak-measurement system. (a) Near-field scanning system in the anechoic chamber. The incident wave is launched from an X-band horn waveguide. (b) Monopole for probing the electric field.

## 4. Experimental setup

A near-field scanner system is designed and built to operate at frequencies between 6 and 12 GHz. It is composed of two parallel conducting plates, each with a diameter of 1 m and spaced 15 mm apart. Holes have been drilled in the top plate, which rotates at intervals that give a resolution of 5 mm. A monopole measures the fields between the two plates at each interval, while a wave is incident from a fixed X-band waveguide (single-mode operational frequency range: 8.2–12.4 GHz; cutoff frequency: 6.557 GHz). Due to diffraction, the wave will be incident on the perturbation from a range of incident angles. A lensing system would mitigate this and allow incidence from a single direction; however, for the purpose of demonstrating multi-incidence cloaking, this setup is suitable. Absorber material is present at the boundaries of the system in order to reduce scattering and reflections from the edges. The experimental setup is shown in figure 3.

## 5. Results and discussion

Simulations are first used to test the performance of the cloak. A waveguide is used to feed the incident wave, with the amplitude and phase of the fields measured throughout the 2D plane. The wavefronts are clearly visible, with a slight diffraction due to the edges of the waveguide. Simulations are then run with the perturbation—an electrically large metallic object exposed and finally cloaked within the system. The simulated scattered fields over a range of angles are shown in figure 4, at both 4 and 9 GHz. Figures 4(a) and (d) compare the fields for the empty system to those of the perturbed system, with the differences between the two cases shaded. It is evident that there is a significant change in the scattered field due to the perturbation. In the cloaked cases, however, shown in figures 4(b) and (e), the scattering profile is reformed to very closely match that of the empty system. Furthermore, the 2D field amplitude plots in figures 4(c) and (f) show little distortion due to the cloaked perturbation, with the wavefronts clearly visible. This confirms the properties of the electromagnetic cloak in simulation.

The measurement setup is then used to verify the performance of the cloak. Due to the limitations of the scanning system and specifically the use of an X-band waveguide, the performance of the cloak could only be tested from 7 GHz (limitation due to the cutoff

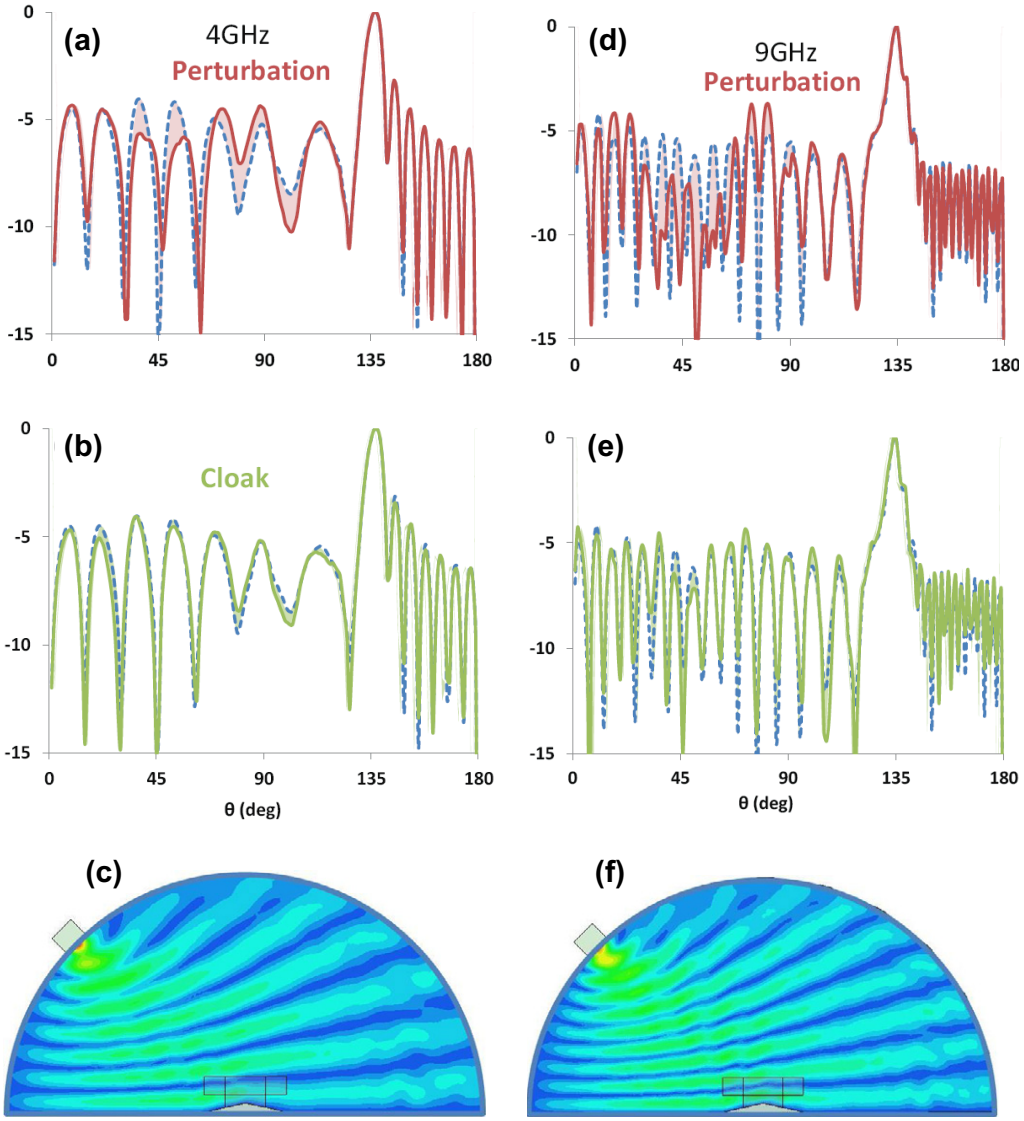


**Figure 4.** Simulated cloaking performance. The performance of the cloak has been tested with full-wave simulations at 4 GHz (a–c) and 9 GHz (d–f). The normalized electric field (solid line) in decibel scale is shown with the perturbation only (a, d) and with the cloaked perturbation (b, e). The dashed line in both cases represents the empty system (no perturbation). To highlight the variations between the cases, the area between the curves has been shaded. It is evident that the structure is successful in cloaking the perturbation. 2D electric field plots are also shown of the cloaked perturbation (c, f), where again it is evident that there is little distortion of the incident electromagnetic waves. Linear scale plots are shown in supplementary figure S6 available from stacks.iop.org/NJP/13/103023/mmedia.

frequency) to 12 GHz (due to multi-mode operation). The near-field scanner is tested first with an empty setup. The measured 2D field amplitude plot is shown in figure 5(a), with the well-formed wavefronts visible. Figure 5(b) represents the measured fields when the perturbation has

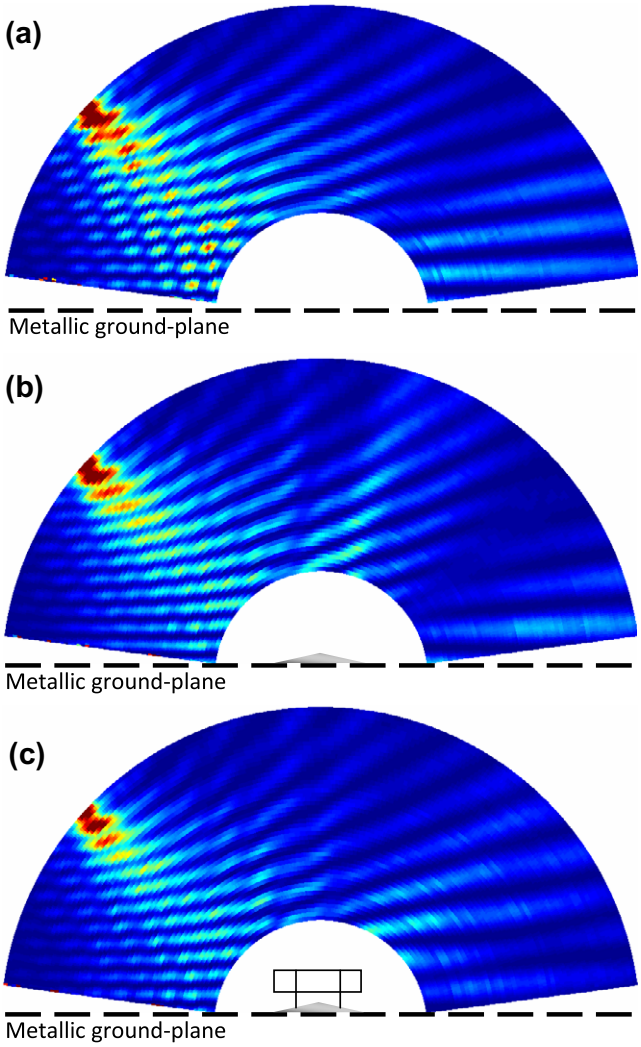


**Figure 5.** Measured electric fields. The electric fields measured in the near-field scanning system are shown. Due to the setup of the scanning system, a semicircular region in which the perturbation and cloak are placed cannot be scanned and is left blank. (a) The empty system (no perturbation or cloak), showing only the incident wave reflecting off of the metallic ground plane. (b) The perturbation resting on the ground plane. (c) The cloaked perturbation. Strong scattering is evident with the perturbation. The cloak significantly reduces the scattering due to the perturbation, with the resulting field distribution similar to that of the perturbation-free system.

been introduced. In this case, the effect on the incoming wave is clearly evident, with scattering and diffraction leading to at least two visibly separate paths of the reflected waves.

The goal of the cloaking material is to 'hide' the electrically large metallic perturbation; reconstructing the scattered waves so that they appear identical to those of the empty scanner. To accomplish this, the dielectric materials are ordered around the object, as in figure 1(b). In the measurements shown in figure 5(c), it is clear that, in contrast to the perturbed case, the

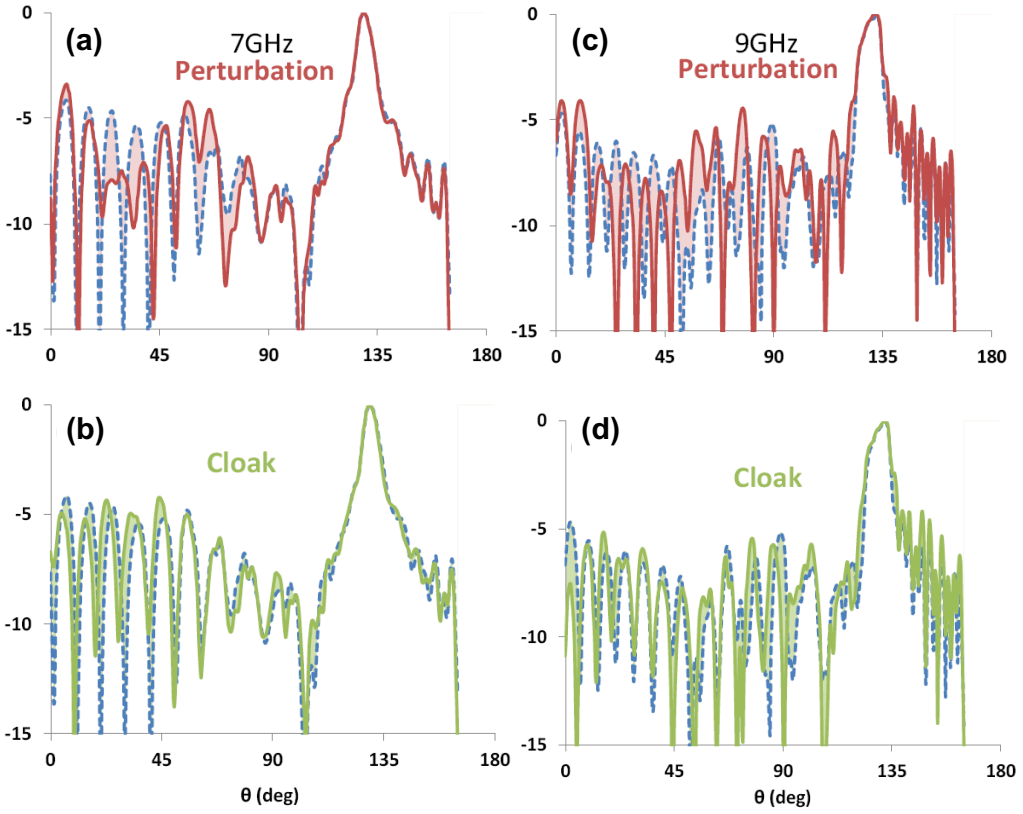


**Figure 6.** Measured cloaking performance at 7–9 GHz (decibel scale). The performance of the fabricated cloaking structure was tested using the described system. The performance at the lower operating frequency range of the near-field scanning system is shown here. The normalized electric fields are plotted at 7 GHz (a, b) and 9 GHz (c, d). Scattering with the perturbation (solid) is compared with that in the empty system (dashed) in (a, c), where in both cases the differences are shaded, and the effects of the perturbation are clearly evident. Similarly, in (b, d) the cloaked perturbation (solid) is compared with the empty system, with significant improvement over the uncloaked case, over almost the entire range of incident angles. Linear scale plots are shown in supplementary figure S7 available from stacks.iop.org/NJP/13/103023/mmedia.

scattered fields appear less affected by the block; the two separate scattered beams are no longer visible, and the wavefront profile appears very similar to that of the empty scanner.

To better analyse the performance of the cloak, the fields are plotted as a function of the scattering angle at the lower half of the frequency band (7 and 9 GHz) in figure 6 and then at the upper range of the frequency band (11 and 12 GHz) in figure 7. Again, the perturbed and the cloaked cases are compared with the empty scanner, with the differences in the field profiles shaded. In figure 6, the measured field profile of the perturbation changes significantly over the range of incidences, as compared to the empty scanner. However, the improvement due to the introduction of the cloak is clearly evident. At the higher frequencies in figure 7, the cloak is again successful in reconstructing the scattering profile of the empty scanner, although performance degrades at more oblique incidences ($\theta \approx 0$–$45^\circ$), in common with

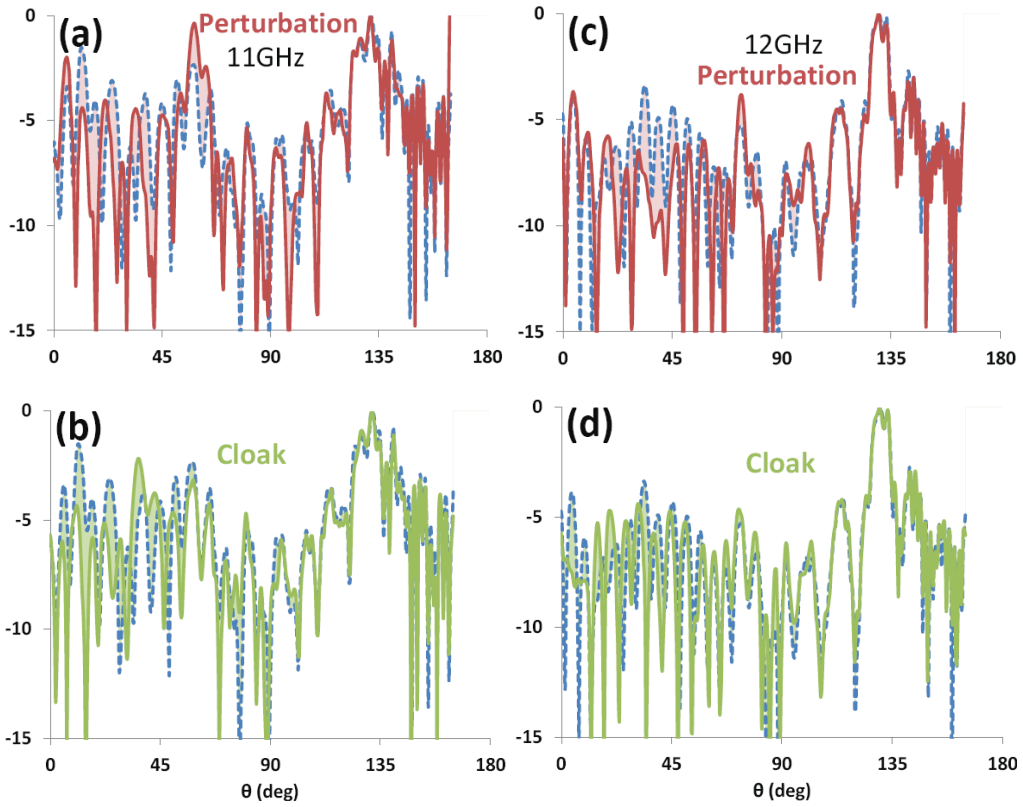


**Figure 7.** Measured cloaking performance at 11–12 GHz (decibel scale). The performance of the fabricated cloaking structure at the higher operating frequency range of the near-field scanning system is shown here. The normalized electric fields are plotted at 11 GHz (a, b) and 12 GHz (c, d). Scattering with the perturbation (solid) is compared with that in the empty system (dashed) in (a, c), where in both cases the differences are shaded, and again the effects of the perturbation are clearly evident. Similarly, in (b, d) the cloaked perturbation (solid) is compared with the empty system. Again, there is significant improvement over the uncloaked case over a large range of incident angles. However, at oblique incidences below about 45°, the cloak does not significantly improve performance as compared to the uncloaked perturbation. Linear scale plots are shown in supplementary figure S8 available from stacks.iop.org/NJP/13/103023/mmedia.

cloaking structures presented in other studies. We note that as the perturbation appears larger electrically at these frequencies, the scattering it causes is more pronounced. The scattered beam at about 60° is particularly visible at 11 GHz, but is well hidden once the cloaking composites are introduced, demonstrating the effectiveness of this scheme, even at higher frequencies. Table 1 quantifies the differences between the measured field profiles, over the two angular ranges: 0–45° and 45–90°. It is evident that while the improvement is not significant at the oblique angles, the cloak successfully and consistently hides the perturbation in the 45–90° range and at all measured frequencies.

**Table 1.** Maximum difference (a.u.) over an angular range between the reference (empty system) and the perturbation (uncloaked and cloaked). A moving average is performed over a waveform (the distance between two peaks), and the maximum over 0–45° and 45–90° is given below.

| $f$ (GHz) | 0–45° | | 45–90° | |
|---|---|---|---|---|
| | Perturbation | Cloak | Perturbation | Cloak |
| 7 | 0.08 | 0.08 | 0.13 | 0.03 |
| 9 | 0.11 | 0.10 | 0.13 | 0.03 |
| 11 | 0.13 | 0.12 | 0.13 | 0.03 |
| 12 | 0.14 | 0.13 | 0.13 | 0.03 |

Furthermore, a higher-resolution discretization may be used to diminish the performance reduction at the more oblique incident angles. Thus, we can conclude that the cloaking material is successful in hiding a wavelength-sized metallic object from an incoming electromagnetic wave. Furthermore, as these dielectrics are non-dispersive (as confirmed by our measurements) and isotropic, this cloaking scheme works over a wide band of frequencies, and for a range of incident angles.

Using the principles of transformation optics, a broadband all-dielectric cloaking device was designed, fabricated and tested for operation at microwave frequencies. The principal advantage of this cloak is that it does not require small-scale substructuring, but is instead made of blocks of polyurethane/$BaTiO_3$ foam composites. Hence, the resulting structure is both low loss and easily fabricated in bulk. Furthermore, due to the random nature and inherently small correlation lengths of the composites, unwanted scattering from the structure of the material is reduced, and effective media approximations for graded dielectrics that are necessary in other approaches (e.g. cylinders or split-ring resonators that are of the order of about $\lambda/10$) are not required.

The dielectric map has been down-sampled to achieve a low-resolution map with a few different dielectric permittivity values. This reduces performance slightly, but simplifies fabrication for practical applications while still providing good cloaking performance over a large range of frequencies. Nevertheless, if the band of operation is to be raised to higher frequencies, the resolution can easily be increased. Furthermore, the procedure presented in this paper may be applied to the development of a range of other transformation optics-based devices. Some optical transformation devices, such as beam expanders [5] and rotators [7], require extreme material properties (less than one), which admittedly may not be realized with the method presented in this paper. However, for many other transformation devices, where no extreme electromagnetic wave behaviour is required, there may only be a small spatial region with dispersive values (less than unity). It has been shown that it will not affect performance significantly if these areas are replaced by air [14, 23]. Furthermore, for certain structures only (approximately) isotropic material parameters may be required, subject to the selection of a proper grid. In this way, it is possible to build optical transformation devices such as planar lens antenna [12–14] and an extraordinary transmission device [11] using the technique presented in this paper. We also note that no truly 3D, perfect electromagnetic cloak has been realized. However, the technique we have presented may be used to produce the 3D cloak in [20].

## Acknowledgments

This work was supported by the Technology Strategy Board, UK under the Collaborative Research and Development programme 'Advanced Materials for Ubiquitous Leading-edge Electromagnetic Technologies' (no. TP/8/ADM/6/1/Q2084L). We thank C G Parini for his assistance in designing and developing the measurement system; J Vazquez and M Philippakis for their useful discussions; and J Dupuy and T Stone for their assistance with fabrication.

## References

[1] Leonhardt U 2006 Optical conformal mapping *Science* **312** 1777–80
[2] Pendry J B, Schurig D and Smith D R 2006 Controlling electromagnetic fields *Science* **312** 1780–2
[3] McCall M W *et al* 2011 A spacetime cloak, or a history editor *J. Opt.* **13** 024003
[4] Ginis V *et al* 2010 Frequency converter implementing an optical analogue of the cosmological redshift *Opt. Express* **18** 5350–5
[5] Rahm M *et al* 2008 Optical design of reflectionless complex media by finite embedded coordinate transformations *Phys. Rev. Lett.* **100** 063903
[6] Chen H Y, Chan C T and Sheng P 2010 Transformation optics and metamaterials *Nat. Mater.* **9** 387–96
[7] Chen H *et al* 2009 Design and experimental realization of a broadband transformation media field rotator at microwave frequencies *Phys. Rev. Lett.* **102** 183903
[8] Greenleaf A *et al* 2009 Cloaking devices, electromagnetic wormholes, and transformation optics *Siam Rev.* **51** 3–33
[9] Lai Y *et al* 2009 Complementary media invisibility cloak that cloaks objects at a distance outside the cloaking shell *Phys. Rev. Lett.* **102** 093901
[10] Wee W H and Pendry J B 2009 Shrinking optical devices *New J. Phys.* **11** 073033
[11] Bao D *et al* 2010 Experimental demonstration of broadband transmission through subwavelength aperture *Appl. Phys. Lett.* **97** 134105
[12] Mei Z, Bai J and Cui T 2011 Experimental verification of a broadband planar focusing antenna based on transformation optics *New J. Phys.* **13** 063028
[13] Yang R, Tang W and Hao Y 2011 A broadband zone plate lens from transformation optics *Opt. Express* **19** 12348–55
[14] Tang W *et al* 2010 Discrete coordinate transformation for designing all-dielectric flat antennas *IEEE Trans. Antennas Propag.* **58** 3795–804
[15] Hao Yang and Mittra Raj 2008 *FDTD Modeling of Metamaterials: Theory and Applications* (Boston, MA: Artech House)
[16] Schurig D *et al* 2006 Metamaterial electromagnetic cloak at microwave frequencies *Science* **314** 977–80
[17] Liu R *et al* 2009 Broadband ground-plane cloak *Science* **323** 366
[18] Tretyakov S *et al* 2009 Broadband electromagnetic cloaking of long cylindrical objects *Phys. Rev. Lett.* **103** 103905
[19] Edwards B *et al* 2009 Experimental verification of plasmonic cloaking at microwave frequencies with metamaterials *Phys. Rev. Lett.* **103** 153901
[20] Ma H F and Cui T J 2010 Three-dimensional broadband ground-plane cloak made of metamaterials *Nat. Commun.* **1** 21
[21] Zhou F *et al* 2010 Three-dimensional cloaking device operates at terahertz frequencies arXiv:1003.3441
[22] Zhou F *et al* 2011 Hiding a realistic object using a broadband terahertz invisibility cloak arXiv:1105.0378
[23] Valentine J *et al* 2009 An optical cloak made of dielectrics *Nat. Mater.* **8** 568–71
[24] Gabrielli L H *et al* 2009 Silicon nanostructure cloak operating at optical frequencies *Nat. Photonics* **3** 461–3
[25] Ergin T *et al* 2010 Three-dimensional invisibility cloak at optical wavelengths *Science* **328** 337–9
[26] Chen X *et al* 2011 Macroscopic invisibility cloaking of visible light *Nat. Commun.* **2** 176

[27] Li J and Pendry J B 2008 Hiding under the carpet: a new strategy for cloaking *Phys. Rev. Lett.* **101** 203901
[28] Kallos E, Argyropoulos C and Hao Y 2009 Ground-plane quasicloaking for free space *Phys. Rev.* A **79** 63825
[29] Nicolson A M and Ross G F 1970 Measurement of the intrinsic properties of materials by time-domain techniques *IEEE Trans. Instrum. Meas.* **19** 377–82
[30] Weir W B 1974 Automatic measurement of complex dielectric constant and permeability at microwave frequencies *Proc. IEEE* **62** 33–6